Single cGMP-activated Ca^{2+}-dependent Cl^- channels in rat mesenteric artery smooth muscle cells

A. S. Piper and W. A. Large

Department of Basic Medical Sciences, Pharmacology and Clinical Pharmacology, Cardiovascular Research Group, St George's Hospital Medical School, Cranmer Terrace, London SW17 0RE, UK

The present study describes the single channel properties of a novel cGMP-activated Ca^{2+}-dependent Cl^- channel in rat mesenteric artery smooth muscle cells. Single channel currents were recorded in cell-attached patches in the presence of 8Br cGMP in response to the addition of caffeine or noradrenaline and in both outside-out and inside-out patches when the internal patch surface was bathed in cGMP and Ca^{2+}. The channels were permeable to Cl^- ions with an anion permeability sequence of SCN^- (1.7) > Cl^- (1.0) > I^- (0.6). Single channel mean open probability (NP_o) was independent of voltage and the channels displayed three conductance levels of 15, 35 and 55 pS. cGMP was required for channel activation and the single channel NP_o increased sharply with raised $[Ca^{2+}]_i$, maximal activation occurring at a $[Ca^{2+}]_i$ of about 100 nM. The relationship between NP_o and cGMP concentration was voltage independent and could be fitted by the Hill equation giving a K_d of about 3 μM and a Hill coefficient (n_H) of 3. cGMP- and Ca^{2+}-dependent channel currents were inhibited by 10 μM $ZnCl_2$ but niflumic acid, an inhibitor of Ca^{2+}-activated Cl^- channels, had no effect. Inhibition of cGMP-dependent protein kinase activity by the cGMP-dependent protein kinase inhibitor KT5823 or replacement of ATP by AMP-PNP reduced NP_o, while activation of cGMP-dependent protein kinase by guanosine 3′, 5′-cyclic monophosphate, β-phenyl-1, N^2-etheno-8-bromo-sodium salt (8Br PET cGMP) produced a significant increase in single channel NP_o. It is likely that these single channel currents underlie the noradrenaline-activated inward current important for vasomotion in these resistance arteries.

(Received 4 November 2003; accepted after revision 19 December 2003; first published online 23 December 2003)
Corresponding author A. S. Piper: Department of Basic Medical Sciences, Pharmacology and Clinical Pharmacology, Cardiovascular Research Group, St George's Hospital Medical School, Cranmer Terrace, London SW17 0RE, UK.
Email: a.piper@sghms.ac.uk

Ca^{2+}-activated Cl^- channels are expressed in the sarcolemma of many different types of smooth muscle cells (Large & Wang, 1996). Since the Cl^- equilibrium potential in smooth muscle is about −20 to −30 mV, stimulation of Ca^{2+}-activated Cl^- currents ($I_{Cl(Ca)}$) evokes depolarization and there is now much evidence to show that $I_{Cl(Ca)}$ contributes to agonist-induced contraction in several smooth muscle preparations (see review by Large *et al.* 2002).

Previously, by comparing the properties of whole-cell currents (e.g. pharmacology, relative anion permeability and voltage dependence), we had considered the characteristics of $I_{Cl(Ca)}$ in different smooth muscle preparations to be sufficiently similar to conclude that there may be a single type of $I_{Cl(Ca)}$ in smooth muscle (Large & Wang, 1996). However, recently, evidence has been provided to indicate that there is another type of Ca^{2+}-dependent Cl^- current in smooth muscle. Thus Peng *et al.* (2001), in a study on vasomotion in rat mesenteric arterioles, described a cGMP-dependent Ca^{2+}-activated inward current. Moreover, the same group have demonstrated that this is a Cl^- conductance which appears to possess several characteristics (e.g. pharmacology and relative halide permeability) that are different to the 'classical $I_{Cl(Ca)}$' in smooth muscle (Matchkov *et al.* 2003). However, this work was carried out on whole-cell currents and much weight for a different Ca^{2+}-dependent Cl^- conductance would be provided from a study on the biophysical characteristics of single channel currents.

In the present investigation we describe the properties of single cGMP- and Ca^{2+}-dependent Cl^- channel currents in rat mesenteric arterioles for comparison with the characteristics of 'classical' single $I_{Cl(Ca)}$ channel currents which we have previously described in rabbit pulmonary artery myocytes (Piper & Large, 2003). This study shows that the Cl^- channels in both

 DOI: 10.1113/jphysiol.2003.057646

vascular preparations have markedly different biophysical properties. In mesenteric arteriolar myocytes intracellular cGMP is an essential prerequisite for channel opening whereas in the pulmonary artery myocytes are activated by an increase in intracellular $[Ca^{2+}]_i$ in the absence of cGMP (Piper & Large, 2003).

Methods

Preparation of mesenteric artery smooth muscle myocytes

All experiments were performed on freshly dispersed rat mesenteric artery smooth muscle myocytes. Male Sprague-Dawley rats weighing 200–250 g were stunned and killed by cervical dislocation as approved under Schedule 1 of the UK Animals (Scientific Procedures) Act 1986, and the mesenteric vascular bed excised. Single smooth muscle cells were isolated as described below. The arterioles were dissected free of fat and connective tissue and single smooth muscle cells were dispersed by treatment with papain and collagenase. Sections of small arteries from the first, second and third branches of the main mesenteric artery were opened along the longitudinal axis and the endothelium removed by gentle rubbing. The tissue strips were placed in a solution containing (mM): NaCl (120); KCl (6); $MgCl_2$ (1.2); $CaCl_2$ (0.05); 4-(2-hydroxy-ethyl)-1-piperazine ethanesulphonic acid (Hepes) 10; glucose (11); pH was adjusted to 7.2 with NaOH, and papain (1 mg l^{-1}), collagenase IA (1–1.5 mg l^{-1}), bovine serum albumin (5 mg l^{-1}) and dithiothreitol (2.5 mM) were added. The tissue was then incubated at 37°C for 25–30 min. Single cells were then isolated by trituration with a fire-polished wide bore pipette. Drops of the resultant cell suspension were placed on glass coverslips and stored at 4°C for up to 4–6 h prior to an experiment.

Solutions

In order to record single cGMP-activated Cl^- currents in the cell-attached recording mode cells were superfused with a solution of the following composition (mM): NaCl (126); $MgCl_2$ (1.2); $CaCl_2$ (1.5); Hepes (10); glucose (11); pH was adjusted to 7.2 with NaOH. The pipette solution for cell-attached patches contained (mM): *N*-methyl-D-glucamine chloride (NMDGCl; prepared by equimolar addition of NMDG and HCl, 126); $MgCl_2$ (1.2); $CaCl_2$ (10); Hepes (10); pH was adjusted to 7.2 with NMDG or HCl as appropriate. The K^+ channel blockers TEA (10 mM) and 4-aminopyridine (4-AP, 10 mM) were added to the pipette solution used for all cell-attached patches in order to block any K^+ channels present. For recordings from excised inside-out patches symmetrical NMDGCl solutions were used. The pipette solution was identical to the NMDGCl-based pipette solution used for cell-attached patches, while the external solution (intracellular surface of patch) contained (mM): NMDGCl (126); $MgCl_2$ (1.2); EGTA (0.1 or 1); MgATP (1); pH was adjusted to 7.2 with NMDG or HCl as appropriate. Both external and pipette solutions contained TEA (10 mM) and 4-AP (10 mM). Varying amounts of $CaCl_2$ (6.8 μM, 65 μM, 256 μM with 1 mM EGTA and 41 μM or 78 μM with 0.1 mM EGTA) were added to the solution in order to buffer free Ca^{2+} to ~1 nM, 10 nM, 50 nM, 100 nM or 1 μM, respectively (calculated using Eqcal for Windows).

For the experiments using excised outside-out membrane patches to record single cGMP-activated Cl^- channel currents the pipette solution had the following composition (mM): NMDGCl (126); Hepes (10); $MgCl_2$ (1.2); EGTA (0.1); MgATP (1); cGMP (0.01); pH was adjusted to 7.2 with NMDG or HCl. $CaCl_2$ was added to the solution at a concentration of 41 μM to give a final Ca^{2+} concentration of 100 nM (calculated as above). The external face of the outside-out patches was bathed with either a NMDGCl-based solution (containing (mM): NMDGCl (126); $CaCl_2$ (1.5); $MgCl_2$ (1.2); Hepes (10); pH adjusted to 7.2 with NMDG or HCl as appropriate) or a NaCl-based solution as described for cell-attached patches above. In experiments to determine the effect of reduced external Cl^- on the conductance, a NaCl-based external solution was used in which the total Cl^- concentration was reduced to 70 mM by replacement of 60 mM NaCl with 120 mM mannitol. In order to determine the relative anion permeability through single cGMP-activated Cl^- channels, either NaI or NaSCN replaced NaCl in the external solution in an equimolar fashion. TEA (10 mM) and 4-AP (10 mM) were also added to both the pipette and the external solutions for outside-out patches.

Changes in liquid junction potential were minimized by the use of a 150 mM KCl-agar bridge connecting the recording chamber and a side bath containing the intracellular solution.

Papain, collagenase 1A, bovine serum albumin, dithiothreitol, Hepes, NMDG, MgATP, mannitol, NaI, NaSCN, EGTA, cGMP, AMP-PNP and 4-aminopyridine were all supplied by Sigma Aldrich. KT5823, 8Br cGMP and 8Br PET cGMP were supplied by Calbiochem.

Electrophysiological recording

All experiments were carried out at room temperature (20–25°C). Pipettes were pulled from borosilicate glass capilliaries and then heat polished. To improve the signal

to noise ratio, pipettes with a tip resistance of 10–15 MΩ were dipped in Sigmacote (Sigma). The patch membrane potential was generated and single channel currents were recorded using a Heka EPC8 patch clamp amplifier and stored on DAT tapes.

Analysis

Current records were low pass filtered offline at 1 kHz and digitized at 5 kHz. Analysis of channel openings and closings to provide a channel events list was carried out using Fetchan 6, using a 50% threshold crossing analysis. For this analysis, current records were filtered at 1 kHz whenever possible to give a minimum time resolution of around 0.6 ms (twice the filter rise time, T_r). The current thresholds used for analysis were determined from Gaussian distributions fitted to the all points histograms. In patches where the single channels exhibited a mixture of full and subconductance current levels (see later) each level was analysed separately. For each patch, mean single channel open probability (NP_o) was calculated as follows:

$$NP_o = (\Sigma(O_n n)/T),$$

where n represents the number of current levels in the patch (1, 2, 3 ... n), (O_n represents the time spent at each open level (i.e. 1–n) and T is the total recording time.

The relationship between NP_o and $[Ca^{2+}]_i$ for inside-out patches was fitted by the Hill equation

$$y = y_{max}\left(x^{nH}/K_d + x^{nH}\right),$$

where y_{max} represents maximum NP_o, K_d is the apparent dissociation constant and n_H is the Hill coefficient.

In order to generate open time and closed time distributions, channel events were grouped into 1 or 2 ms bins, respectively, and the resultant distributions were fitted by exponential functions using pSTAT 6 software.

Results

Properties of single cGMP- and Ca^{2+}-dependent channel currents recorded in cell-attached patches

At rest, when the applied patch voltage was +50 mV (i.e. patch hyperpolarized by 50 mV in addition to the cell resting membrane potential), no spontaneous single channel currents were observed in recordings from 10 cell-attached patches in rat mesenteric artery smooth muscle cells (Fig. 1*A*). In 56% (5 of 9) of cell-attached patches single channel currents with a low NP_o (0.07 ± 0.03) were observed when cells were exposed to the cell-permeable cGMP analogue 8Br cGMP (300 μM) alone (Fig. 1*A*). In the presence of 300 μM 8Br cGMP the addition of caffeine (10 mM) markedly increased single channel activity and these currents had a mean single channel conductance of 20 ± 3 pS ($n = 6$). The NP_o of these channels appeared to be independent of applied voltage and was 0.21 ± 0.05 and 0.19 ± 0.04 ($n = 6$; $P > 0.05$, paired t test) when the applied patch voltage was +50 mV and −50 mV, respectively. In addition, when cells were exposed to caffeine (10 mM) alone, occasional single channel currents with a low total single channel open probability (NP_o ~0.01) were recorded in 33% (2 of 6) patches.

Single channel currents were also activated by noradrenaline (NA) in the presence of 300 μM 8Br cGMP (e.g. Fig. 1*B*; $n = 3$). Upon close inspection of individual current records it was evident that, with either caffeine or NA, at least two separate conductance levels could be discerned (Fig. 2*A*). The amplitude of the larger conductance level was around 20–25 pS but there was also a subconductance level with an amplitude of around 10–15 pS. The larger current level was not simply a double opening of the smaller current level as distinct transitions between the closed level and both open levels could be observed.

Figure 2*A* shows traces of current recorded from a cell-attached patch when a range of voltages was applied and both conductance levels described above could be distinguished at each voltage. The resultant current–voltage (I–V) relationship for each of the current levels (Fig. 2*B*) reversed close to the resting membrane potential of the cell and the relationship tended towards an 'S' shape with outward and inward rectification at extreme negative and positive potentials, respectively. The smaller conductance level had a mean amplitude of 12 ± 1 pS, as estimated from the slope conductance of the linear portion of the I–V curve, while the larger conductance had an amplitude of 25 ± 4 pS ($n = 6$). A more detailed study of the different conductance levels displayed by cGMP-activated Cl^- channels is described below.

Properties of single cGMP- and Ca^{2+}-dependent channel currents recorded in outside-out patches

Figure 3*A* shows a trace of single channel currents recorded from an outside-out patch at a holding potential of −50 mV. The patch was bathed with NMDGCl-based solutions with 140 mM Cl^- either side of the membrane. The pipette solution contained 10 μM cGMP, 1 mM MgATP and 100 nM Ca^{2+} which produced single channel activity with an NP_o similar to that recorded in cell-attached patches with 300 μM 8Br cGMP and 10 mM caffeine. As described for cell-attached patches the NP_o for

single cGMP and Ca^{2+}-dependent channels was voltage independent (NP_o was 0.25 ± 0.05 and 0.19 ± 0.04 at −50 mV and +50 mV, respectively, $n = 10$, $P > 0.05$, paired t test). It is clear that there are three separate current levels present in this recording, and that transitions between the closed level (continuous line) to each of the three current levels can be seen, suggesting that they are not simply multiple openings. The all points histogram taken of these data is shown in Fig. 3*B*. The first peak with a mean amplitude of 0 pA represents the closed current level, while there were three further peaks representing open channel states with amplitudes of −0.82, −1.71 and −2.75 pA. Figure 3*C* shows the mean *I–V* curves from several outside-out patches for each conductance level. The *I–V* relationships showed a slight degree of inward and outward rectification at extreme negative and positive voltages, respectively. The slope conductances estimated from the linear portion of the *I–V* relationships were 17 ± 2 pS ($n = 14$), 37 ± 5 pS ($n = 9$) and 53 ± 5 pS ($n = 5$), respectively. The smallest subconductance level was present in all outside-out patches at all the voltages tested. However, openings to the intermediate and full conductance levels did not occur at every voltage tested. There appeared to be no correlation between the absence or presence of channel transitions to the intermediate or full conductance level in each patch with either NP_o or voltage.

Effect of reduced external Cl^- and halide permeability sequence for cGMP- and Ca^{2+}-dependent channels in outside-out patches

With the recording conditions used in this study, it was likely that the single cGMP- and Ca^{2+}-dependent channel currents recorded in cell-attached and outside-out patches represented a Cl^- conductance. In order to confirm this a series of experiments was carried out using outside-out membrane patches that allowed either the reduction or replacement of external chloride ions. When the main external cation was $NMDG^+$ the mean conductance of the three levels described above estimated from the linear portion of each *I–V* curve was 17 ± 2 pS ($n = 14$), 34 ± 5 pS ($n = 9$) and 53 ± 5 pS ($n = 5$) and the *I–V* curves reversed at 1 ± 3 mV ($n = 14$), 4 ± 4 mV ($n = 9$) and −1 ± 4 mV, respectively. When external Cl^- was reduced to 70 mM by the replacement of NaCl by 120 mM mannitol,

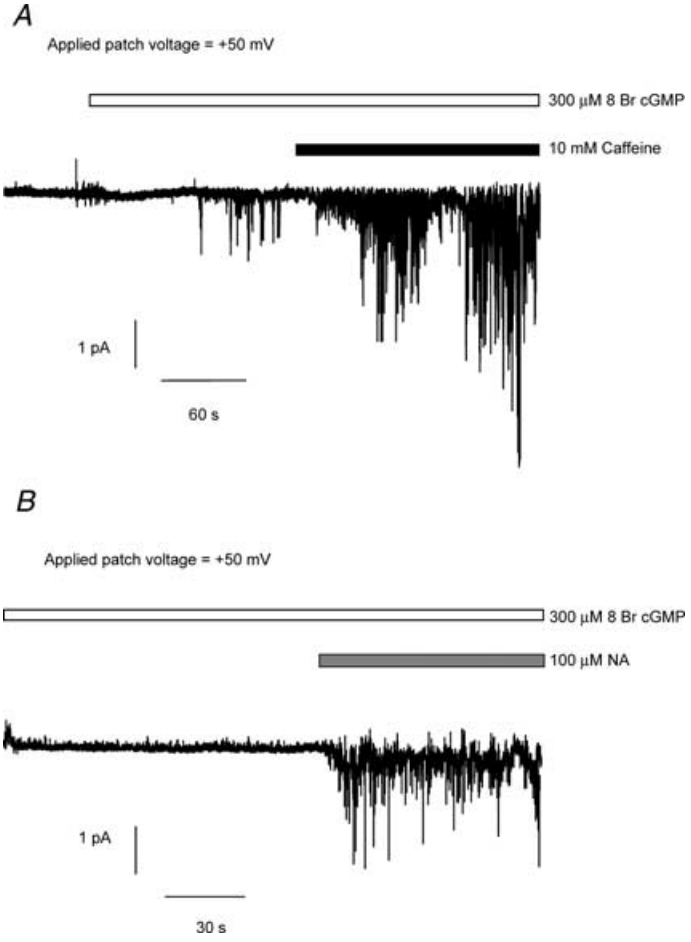

Figure 1. Single cGMP- and Ca^{2+}-dependent Cl^- channel currents recorded in a cell-attached patch
A shows current recorded at an applied patch potential of +50 mV (50 mV hyperpolarization in addition to the cell resting membrane potential) at rest, in the presence of 8Br cGMP (300 μM, open bar) and caffeine (10 mM, filled bar). *B* is a trace of single channel currents recorded from a second cell-attached patch with an applied patch potential of +50 mV in the presence of 8Br cGMP (300 μM, open bar) and noradrenaline (NA, 100 μM, shaded bar). In this and subsequent figures the current traces have been reversed where necessary such that inward currents appear as a downward deflection and outward currents as an upward deflection.

the amplitude of each conductance level was 18 ± 2 pS (n = 4), 34 ± 3 pS (n = 3) and 49 ± 5 pS (n = 3), respectively. However, there was a significant shift in reversal potential (V_{rev}) for each conductance level to +12 ± 1 mV (n = 4), +17 ± 2 mV (n = 3) and +17 ± 3 mV (n = 3, $P < 0.05$, unpaired t test). This compares favourably with the shift in V_{rev} predicted for a Cl^- conductance by the Nernst equation (+17 mV).

Experiments were then carried out to determine the relative anion permeability through cGMP- and Ca^{2+}-dependent Cl^- channels by bathing outside-out patches in solutions containing 126 mM NaCl, NaSCN or NaI. Table 1 shows the amplitude of each of the single channel conductance levels and also the V_{rev} for each level. There was no significant change in the amplitude of each current level while V_{rev} for each current level was shifted by around −15 mV in NaSCN and by around +10 mV in NaI. The permeability sequence and ratios were therefore SCN^- (1.7) > Cl^- (1) > I^- (0.6).

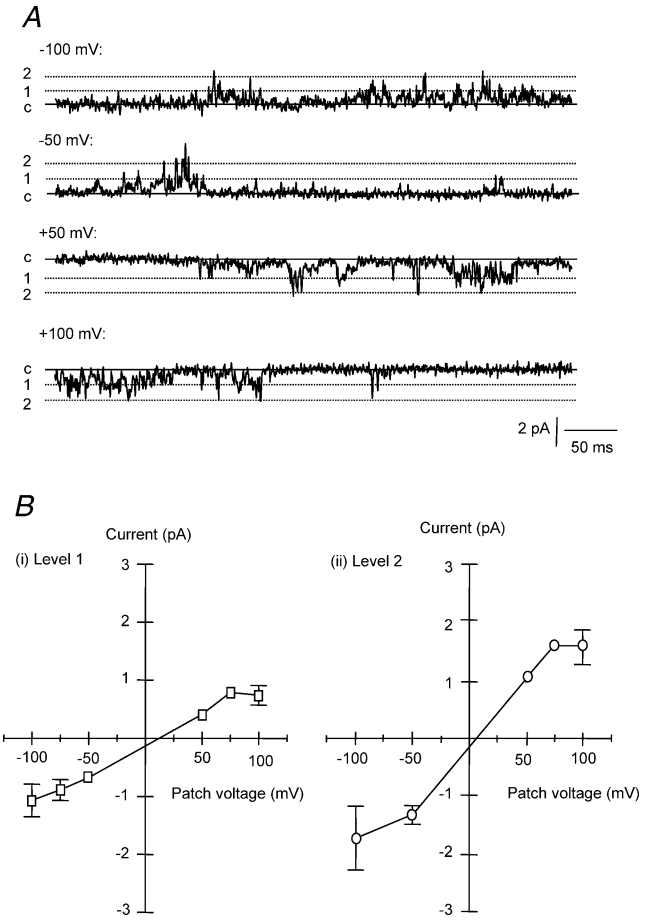

Figure 2. Single cGMP- and Ca^{2+}-dependent Cl^- channel currents recorded at a range of applied patch voltages in a cell-attached patch

A shows currents recorded at applied patch potentials between −100 mV and +100 mV after caffeine (10 mM) and 8Br cGMP (300 μM) were applied to the cell. Continuous lines represent the closed channel current level (c) while the dotted lines denote the two conductance levels (1 and 2). *B*, mean *I–V* relationship for the smaller subconductance level (□ n = 5) and the larger subconductance level (○; n =5). Data are mean ± S.E.M.

Comparison of single channel data recorded with different configurations

There was no significant difference in the mean amplitude of each of the three current levels described above

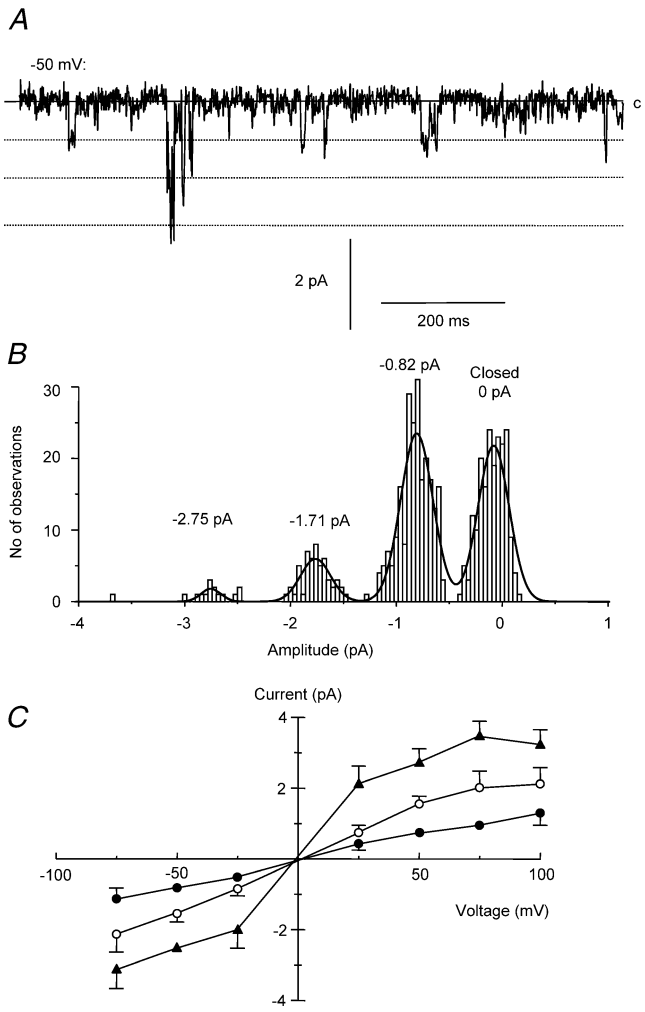

Figure 3. Full conductance and subconductance openings of single cGMP- and Ca^{2+}-dependent Cl^- channels in outside-out patches

A shows a trace of single channel currents recorded from an outside-out patch at −50 mV with 10 μM cGMP and 100 nM $[Ca^{2+}]_i$ in the pipette solution. The continuous line represents the closed channel level (c), while the dotted lines denote the channel subconductance and full conductance levels. *B* is an all points histogram taken from the current trace shown in *A*. The bin width was 0.04 pA and the data were fitted by the sum of four Gaussian curves, with means of 0, −0.82, −1.71 and −2.75 pA, respectively. *C*, mean single channel *I–V* relationships for subconductance and full conductance openings of single cGMP-activated Cl^- channels in the presence of 10 μM cGMP and 100 nM $[Ca^{2+}]_i$. Data are mean ± S.E.M., n = 4–6.

Table 1. Conductance and reversal potential (V_{rev}) values calculated from the *I–V* curves for each conductance level of cGMP- and Ca^{2+}-dependent Cl^- channels recorded in outside-out patches with different external solutions (see text)

	126 mM NaCl		126 mM NaSCN		126 mM NaI	
	Conductance (pS)	V_{rev} (mV)	Conductance (pS)	V_{rev} (mV)	Conductance (pS)	V_{rev} (mV)
Level 1	23 ± 2 ($n = 13$)	$+5 \pm 2$ ($n = 13$)	17 ± 2 ($n = 8$)	-14 ± 5 ($n = 8$)	21 ± 5 ($n = 5$)	$+13 \pm 2$ ($n = 5$)
Level 2	38 ± 5 ($n = 12$)	$+5 \pm 2$ ($n = 12$)	37 ± 5 ($n = 6$)	-9 ± 2 ($n = 6$)	43 ± 4 ($n = 4$)	$+17 \pm 2$ ($n = 4$)
Level 3	66 ± 11 ($n = 7$)	$+4 \pm 3$ ($n = 7$)	61 ± 10 ($n = 4$)	-12 ± 3 ($n = 4$)	64 ± 8 ($n = 4$)	$+17 \pm 5$ ($n = 4$)

Data are mean ± S.E.M., *n* values are shown in parentheses.

between single channel current recorded with either of the configurations used in this study in the presence of external $NMDG^+$. For example, with cell-attached recording (NMDG pipette solution) the amplitude of the first and second current levels were 12 ± 1 pS and 25 ± 4 pS ($n = 6$), respectively (the highest level was not seen often in cell-attached patches), while for outside-out patches with external $NMDG^+$-containing solutions the amplitudes of the current levels were 17 ± 2 pS ($n = 14$; $P > 0.05$, unpaired *t* test), 34 ± 5 pS ($n = 9$; $P > 0.05$) and 53 ± 5 pS ($n = 4$), respectively. With inside-out recording, the amplitude of each conductance level was 15 ± 2 pS ($n = 6$; $P > 0.05$), 34 ± 3 pS ($n = 5$; $P > 0.05$) and 43 ± 9 pS ($n = 4$; $P > 0.05$). Interestingly, the mean amplitude of the single channel currents recorded in outside-out patches was significantly greater with external Na^+ compared to external $NMDG^+$, and with external Na^+ ions the mean amplitude of each conductance level was 23 ± 2 pS ($n = 13$, $P < 0.05$), 46 ± 5 pS ($n = 10$; $P < 0.05$) and 78 ± 11 pS ($n = 6$; $P < 0.05$). There was no significant difference in the V_{rev} for each of the conductance levels which were $+1 \pm 3$ mV ($n = 14$), $+4 \pm 4$ mV ($n = 9$) and -1 ± 4 mV ($n = 5$), respectively, with 126 mM NaCl compared to $+5 \pm 2$ mV ($n = 13$; $P > 0.05$), $+5 \pm 2$ mV ($n = 10$; $P > 0.05$) and $+4 \pm 3$ mV ($n = 5$; $P > 0.05$), respectively, with 126 mM NMDGCl. This suggests that whereas the Cl^- channels do not appear to be permeable to cations, the external cation affects the amplitude of the conductance.

cGMP and Ca^{2+} dependence of chloride channel activation in inside-out patches

The next set of experiments studied the cGMP and Ca^{2+} dependence of the Cl^- channel by using inside-out patches. As can be seen in Fig. 4*A*, it was possible in some patches (3 of 6) to record channel activity in the presence of 10 μM cGMP and very low $[Ca^{2+}]_i$ (~1 nM) and the mean NP_o was 0.002 ± 0.001 ($n = 3$). Subsequent addition of 100 nM $[Ca^{2+}]_i$ markedly increased NP_o to 0.28 ± 0.13 ($n = 6$). NP_o was determined for a range of cGMP concentrations with 100 nM $[Ca^{2+}]_i$ and the data at a patch potential of −100 mV are shown in Fig. 4*B*. The data could be fitted by the Hill equation, giving an estimated maximum NP_o (V_{max}) of 0.3. The K_d, or value of cGMP for 50% of maximum activation, was 2.8 μM, while the Hill coefficient was 2.9, suggesting that the binding of up to three cGMP molecules may be needed to produce channel activation. Similar results were obtained at all the voltages tested (data not shown), suggesting that the binding of cGMP and the resultant Cl^- channel activation is not voltage dependent.

The effect of varying $[Ca^{2+}]_i$ on Cl^- channel activity is shown in Fig. 4*C* and *D*. As can be seen from Fig. 4*C*, although isolated channel openings could occasionally be discerned immediately after patch excision into a solution containing ~1 nM $[Ca^{2+}]_i$, raising $[Ca^{2+}]_i$ to 100 nM could not produce any further activation of single Cl^- channels suggesting that the channels are not Ca^{2+} activated. However, when 10 μM cGMP was added, channel activity increased markedly (Fig. 4*C*). Figure 4*D* shows the effect of varying $[Ca^{2+}]_i$ on the NP_o of single cGMP-activated Cl^- channels. In the presence of 10 μM cGMP at −100 mV, channel activity was steeply Ca^{2+} dependent. Low levels of channel activity were recorded for $[Ca^{2+}]_i$ up to 50 nM, with maximal channel activation when Ca^{2+} was 100 nM, and no further increase when $[Ca^{2+}]_i$ was 1 μM. Similar results were obtained at all voltages tested (data not shown).

These data suggest that the Cl^- channels are activated by cGMP, and that $[Ca^{2+}]_i$ further increases channel activation.

Single channel current open time distribution for cGMP and Ca^{2+}-dependent Cl^- channel currents in inside-out patches

Analysis of single channel open time distributions were studied in inside-out patches at a range of voltages and cGMP concentrations. Figure 5 shows data for the smallest

sublevel as this was the level most likely to be present in each patch, although data from both the intermediate and full conductance levels were similar (data not shown). The log open time distributions for the small amplitude subconductance level of channels activated by 10 μM cGMP with a $[Ca^{2+}]_i$ of 100 nM at −50 mV and +50 mV in a single inside-out patch are shown in Fig. 5*A* and *B*. The distribution could be fitted by a single exponential function to give a single mean open time of 2.1 ms at −50 mV (mean data was 2.0 ± 0.2 ms, $n = 18$) while at +50 mV the mean open time was also about 2 ms (mean data: 2.2 ± 0.3 ms, $n = 18$).

The single channel mean open time for each conductance level was also independent of cGMP concentration. Figure 5*C* and *D* shows the log open time distribution for channels activated by 5 μM or 10 μM cGMP with a $[Ca^{2+}]_i$ of 100 nM at −50 mV. With 5 μM cGMP the open time distribution could be fitted by a single exponential function giving a single mean open time of 2.6 ms (mean data was 1.5 ± 0.2 ms, $n = 8$) while in the same patch with 10 μM cGMP the mean open time was 2.5 ms (mean data was 2.0 ± 0.2 ms, $n = 18$).

These data show that the mean open time for each channel conductance level was neither cGMP nor voltage dependent. Detailed analysis of channel closures was not attempted because the presence of multiple channel subconductance levels made it difficult to determine precisely the presence of only one channel in each patch.

Effect of blockers of Cl^- channels on single cGMP- and Ca^{2+}-dependent channels

First we investigated the effect of niflumic acid (NFA), which is a well-known antagonist of $I_{Cl(Ca)}$. Figure 6*A* shows a trace of current recorded from an outside-out membrane patch in the absence and presence of NFA (100 μM). NFA had no effect on the NP_o of single cGMP-activated Cl^- channels (−50 mV: control $NP_o = 0.14 \pm 0.02$; +NFA $NP_o = 0.18 \pm 0.11$; NFA washout $NP_o = 0.17 \pm 0.09$; $n = 4$). However, whole-cell cGMP-activated Cl^- currents are inhibited by $ZnCl_2$ (Matchkov *et al.* 2003), and as Fig. 6*B* shows, single cGMP-activated channel currents are also blocked by 10 μM $ZnCl_2$. There was a significant reduction in NP_o in the presence of 10 μM $ZnCl_2$ (−50 mV: control $NP_o = 0.19 \pm 0.04$; +$ZnCl_2$ $NP_o = 0.06 \pm 0.02$; $n = 5$, $P < 0.05$, paired t test) which was reversed when $ZnCl_2$ was removed (Fig. 6*B*). We studied the effect of a range of $ZnCl_2$ concentrations and found that a value of

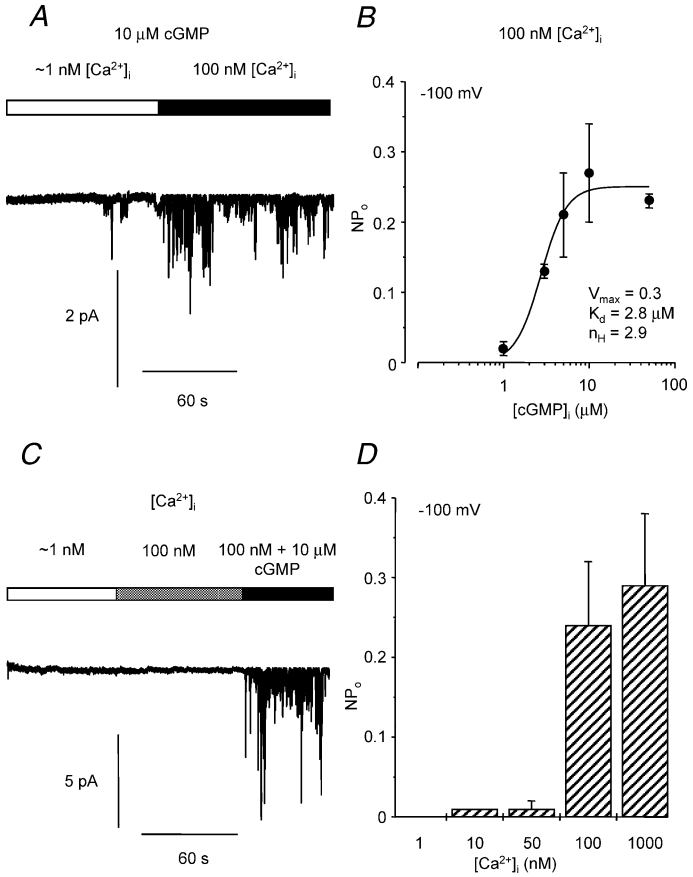

Figure 4. cGMP and Ca^{2+} dependence of cGMP-activated Cl^- channels in inside-out patches
A, trace of current recorded from an inside-out patch in the presence of 10 μM cGMP and ~1 nM $[Ca^{2+}]_i$ (open bar) and 100 nM $[Ca^{2+}]_i$ (filled bar). Note that there was some channel activity with 10 μM cGMP and low $[Ca^{2+}]_i$. *B* is a plot of NP_o *versus* cGMP concentration at a patch potential of −100 mV. Data at each voltage were fitted by the Hill equation to give the apparent dissociation constant (K_d) and the Hill coefficient (n_H). *C* shows a trace of current recorded from a second inside-out patch which was excised into a solution containing ~1 nM $[Ca^{2+}]_i$ (open bar), then 100 nM $[Ca^{2+}]_i$ (shaded bar) and then exposed to 10 μM cGMP (filled bar). *D* is a bar chart to show NP_o at $[Ca^{2+}]_i$ between ~1 nM and 1000 nM in the presence of 10 μM cGMP at a patch potential of −100 mV. Data are mean ± S.E.M., $n = 4$–10.

approximately 6 μM would produce 50% inhibition of the mean single channel open probability.

Effect of protein kinase G inhibition and activation on cGMP-activated Ca^{2+}-dependent Cl^- channels in inside-out patches

The data presented above indicate that cGMP is necessary for Cl^- channel activation, and the following sets of experiments were carried out in order to determine the role of cGMP-dependent protein kinase (protein kinase G) in single channel activation. In cell-attached patches at an applied patch potential of +50 mV the mean single channel NP_o was 0.21 ± 0.05 ($n = 6$) in the presence of 300 μM 8Br cGMP and 10 mM caffeine. When cells were exposed to the protein kinase G inhibitor, KT5823 (1 μM) in the presence of 300 μM 8Br cGMP and 10 mM caffeine there was an 80% reduction in NP_o to 0.04 ± 0.01 ($n = 4$; $P < 0.05$, unpaired t test).

Figure 7*A* shows a trace of current recorded from an inside-out patch exposed to 10 μM cGMP and 100 nM $[Ca^{2+}]_i$ when MgATP was replaced by the non-hydrolysable analogue AMP-PNP as indicated by the hatched bar. When ATP was removed, thus preventing kinase activity, there was a significant decrease in NP_o (−50 mV: control $NP_o = 0.16 \pm 0.02$; +AMP-PNP $NP_o = 0.003 \pm 0.001$, $P < 0.05$, $n = 4$). Similar results were obtained at all voltages tested (data not shown). In two patches the effect of AMP-PNP was reversed on washout.

Replacement of cGMP with the more potent activator of protein kinase G, 8Br PET cGMP, produced a significant increase in single channel NP_o (Fig. 7*B*). At −50 mV with 100 nM $[Ca^{2+}]_i$ in the presence of 10 μM cGMP, single channel NP_o was 0.13 ± 0.02, while in the presence of 10 μM 8Br PET cGMP NP_o was 0.27 ± 0.03 ($P < 0.05$, $n = 4$). Similar results were obtained at all voltages tested (data not shown).

These data suggest that protein kinase G activation is necessary for the opening of cGMP-activated Ca^{2+}-dependent Cl^- channels.

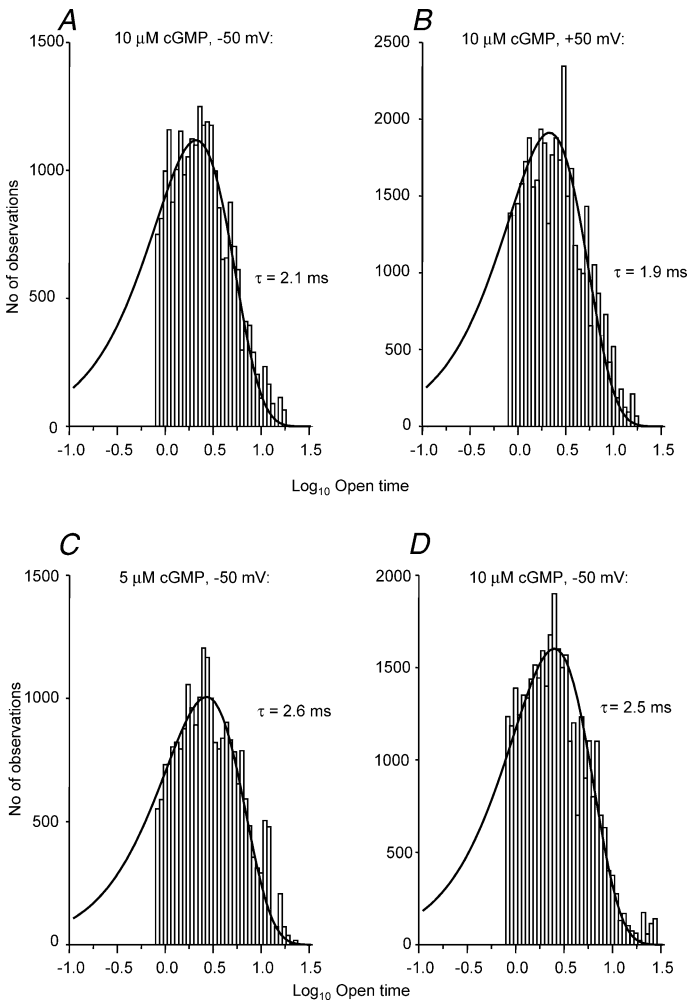

Figure 5. Logarithmic open time distributions of cGMP-activated Cl^- channel currents in inside-out patches
A and *B*, single channel current open time distribution for the smallest subconductance level recorded at, respectively, −50 mV and +50 mV with 10 μM cGMP and 100 nM $[Ca^{2+}]_i$. The logarithm of the open time for channel events was plotted against frequency and the data fitted by a single exponential function with a time constant of about 2 ms. *C* and *D* show the single channel current open time distributions from another inside-out patch with 100 nM $[Ca^{2+}]_i$ and 5 μM and 10 μM cGMP, respectively, at −50 mV. The data were fitted by a single exponential function with a time constant of about 2 ms. In *A*–*D* the log bin width was 0.4.

Additional Cl^- conductances present in these experiments

Channel events characteristic of the 'classical' calcium-activated Cl^- channels described by Piper & Large (2003) in rabbit pulmonary artery myocytes were observed in many patches exposed to raised $[Ca^{2+}]_i$ when the current recordings were filtered at 250 Hz and these channels had a mean conductance of around 3 pS (data not shown). Because of the small amplitude of these channel events they lay below the 50% threshold used for analysis of cGMP-activated single channel currents, and therefore were not included in any of the analysis detailed above.

Discussion

The present study is the first to describe the single channel properties of a novel cGMP-activated Ca^{2+}-dependent Cl^- channel in rat mesenteric artery smooth muscle cells. Single channel activity could be recorded in cell-attached patches, where there is very little perturbation of the intracellular contents, in the presence of the cell-permeable cGMP analogue 8Br cGMP and either caffeine or NA. Similar single channel currents were recorded in both outside-out and inside-out patches. The channels were shown to be permeable to Cl^- ions but not cations and the anion permeability sequence was $SCN^- > Cl^- > I^-$. The channels displayed three conductance levels of around 15, 35 and 55 pS and the maximum mean single channel open probability was around 0.25–0.30 and was independent of voltage.

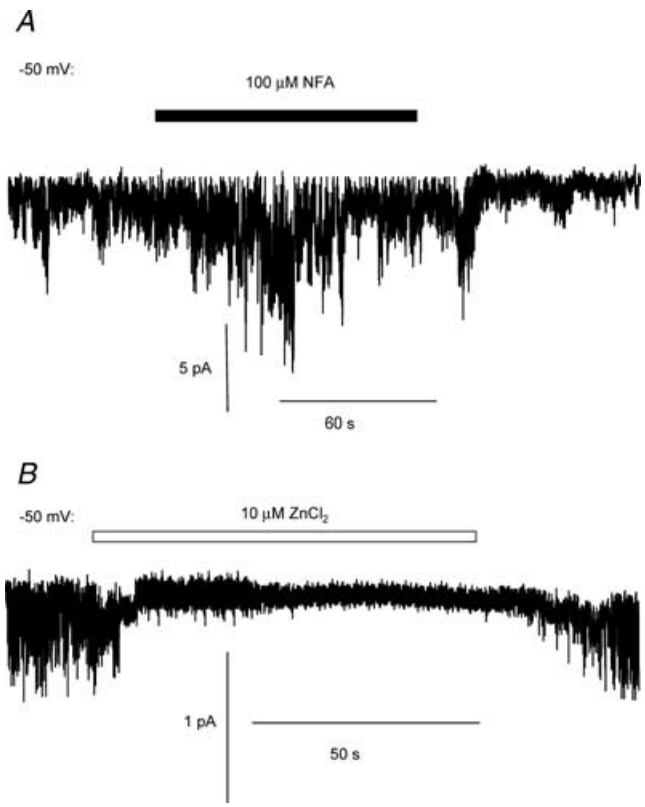

Figure 6. Effect of Cl^- channel blockers on single cGMP-activated Cl^- channel currents in outside-out patches
A shows a trace of current at a patch potential of −50 mV in the absence and presence of niflumic acid (NFA; 100 μM; filled bar). *B*, trace of current from a second outside-out patch at −50 mV in the absence and presence of 10 μM $ZnCl_2$ (open bar).

Comparison of cGMP- and Ca^{2+}-dependent Cl^- channels and Ca^{2+}-activated Cl^- channels

We have recently described the single channel properties of Ca^{2+}-activated Cl^- channels in rabbit pulmonary artery

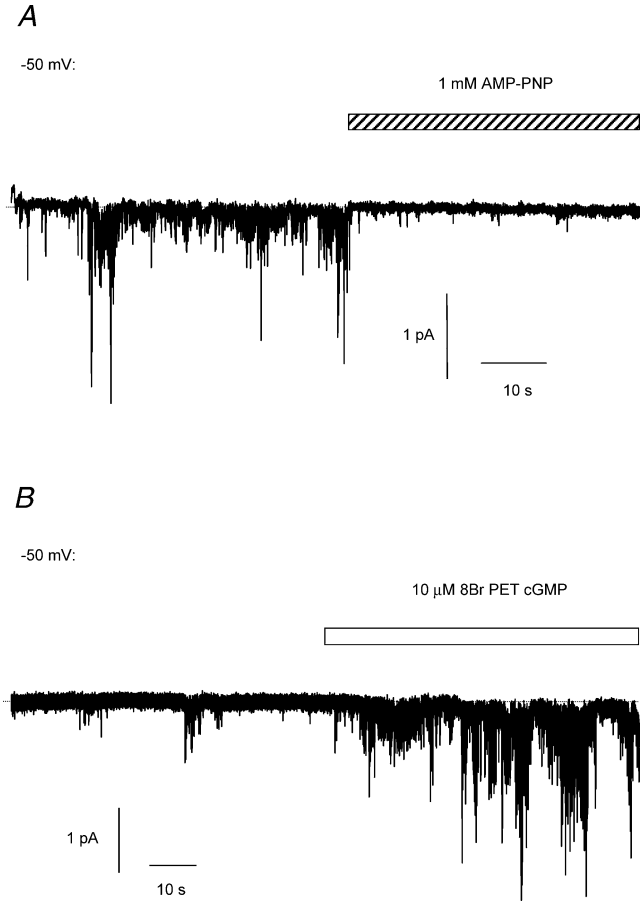

Figure 7. Effect of inhibition or activation of protein kinase G on single cGMP-activated Cl^- channels in inside-out patches
A, trace of single channel currents at a patch potential of −50 mV in the presence of 10 μM cGMP, 100 nM $[Ca^{2+}]_i$ and either 1 mM MgATP or the non-hydrolysable ATP analogue AMP-PNP (1 mM, hatched bar). *B* shows a trace recorded from a second patch at a potential of −50 mV in the presence of 100 nM $[Ca^{2+}]_i$, 1 mM MgATP and either 10 μM cGMP or 10 μM 8Br PET cGMP, a more potent activator of protein kinase G (open bar). Note that there was some channel activity in the presence of cGMP, but single channel NP_o was markedly increased in the presence of 8Br PET cGMP.

smooth muscle cells (Piper & Large, 2003), which are very different from the Cl^- channels described in the present study. The most important difference between these two Ca^{2+}-dependent Cl^- conductances is in their requirement for cGMP. In the present study there was an absolute requirement for cGMP in order to produce channel activation, as channel activity was recorded in the presence of 10 μM cGMP and very low $[Ca^{2+}]_i$ (~1 nM), although single Cl^- channel currents were not recorded in inside-out patches in the absence of cGMP even if $[Ca^{2+}]_i$ was raised to 100 nM. However, in the rabbit pulmonary artery Ca^{2+} is the primary activator of the Cl^- channels and cGMP is not required, although it can increase NP_o (A. S. Piper & W. A. Large, unpublished observations). Activation of cGMP-dependent protein kinase appeared to be an essential step in the activation of cGMP-activated currents as inhibition of kinase activity by either the selective cGMP-dependent protein kinase inhibitor KT5823 in cell-attached patches or replacement of ATP by the non-hydrolysable analogue AMP-PNP in inside-out patches reduced the mean single channel open probability. Also, activation of cGMP-dependent protein kinase by the more potent cGMP analogue 8Br PET cGMP produced a significant increase in single channel NP_o in inside-out patches.

Ca^{2+}-activated Cl^- channels and cGMP-activated Ca^{2+}-dependent Cl^- channels, in common with many Cl^- conductances, display multiple conductance levels. However, the amplitudes of the conductance levels, 1.2, 1.8 and 3.5 pS, respectively, for $I_{Cl(Ca)}$ (Piper & Large, 2003) and 15, 35 and 55 pS for cGMP- and Ca^{2+}-dependent channels are very different. There are also significant differences in the relative halide permeability sequence which was SCN^- (10) > I^- (4.0) > Cl^- (1.0) for $I_{Cl(Ca)}$ (Greenwood & Large, 1999) while in the present study the sequence was SCN^- (1.7) > Cl^- (1.0) > I^- (0.6).

The open probability for single Ca^{2+}-activated Cl^- channels in rabbit pulmonary artery smooth muscle cells was voltage dependent at low $[Ca^{2+}]_i$ (Piper & Large, 2003) and was greater at positive membrane voltages, while for cGMP-activated Ca^{2+}-dependent Cl^- channels NP_o was independent of voltage. The relationship between NP_o and cGMP concentration for cGMP-activated Ca^{2+}-dependent Cl^- channels was voltage independent and could be fitted by the Hill equation giving a K_d of around 3 μM and a Hill coefficient (n_H) of about 3. This suggests that the binding of cGMP and subsequent channel activation is voltage independent, and further, that the binding of at least three cGMP molecules are required for channel activation. The single channel NP_o increased sharply, with $[Ca^{2+}]_i$, maximal activation occurring at a $[Ca^{2+}]_i$ of around 100 nM. However, when NP_o was plotted against $[Ca^{2+}]_i$ for Ca^{2+}-activated Cl^- channels in rabbit pulmonary artery myocytes, both the K_d and the Hill coefficients were voltage dependent, the K_d being 8 nM and 250 nM, and n_H 1.3 and 2.3, at +100 mV and −100 mV, respectively (Piper & Large, 2003).

In the present study, cGMP- and Ca^{2+}-dependent Cl^- channels displayed three conductance levels and each of these levels behaved in a similar manner with regards to their kinetics. The single channel mean open time was around 2 ms for each conductance level and was both voltage and cGMP independent. On the other hand, the distribution of open times for Ca^{2+}-activated Cl^- channels was fitted by two exponentials of about 5 ms and 30 ms that were neither voltage nor Ca^{2+} dependent. Although the openings of cGMP- and Ca^{2+}-dependent Cl^- channels appeared to occur in bursts, conventional analysis of burst duration was not attempted because the presence of multiple conductance levels made it difficult to precisely determine that patches contained only one channel.

NFA, which has been shown to be a selective inhibitor of Ca^{2+}-activated Cl^- channels in rabbit portal vein smooth muscle cells (Hogg *et al.* 1994) had no effect on cGMP-activated Ca^{2+}-dependent channels, while 10 μM $ZnCl_2$ inhibited the single channel currents in outside-out patches. However, Ca^{2+}-activated Cl^- channels in rabbit pulmonary artery smooth muscle cells were blocked by NFA (Piper *et al.* 2002).

All of the differences detailed above indicate that the Ca^{2+}-activated Cl^- conductance present in rabbit pulmonary artery smooth muscle cells, and the cGMP-activated Ca^{2+}-dependent Cl^- conductance described in the present study, represent separate molecular entities. Additionally, it was often possible to record single channel events with similar properties to those described for $I_{Cl(Ca)}$ in inside-out and outside-out patches from rat mesenteric artery, showing that this latter preparation possesses both classes of Cl^- channel.

Comparison of the properties of cGMP-activated Ca^{2+}-dependent channels with cloned Ca^{2+}-dependent Cl^- channels

A family of proteins termed CLCA that act as Ca^{2+}-sensitive Cl^- channels have recently been described and cloned, although a native current with similar properties to the cloned channel currents has yet to be identified. As cGMP- and Ca^{2+}-dependent Cl^- channels are significantly different from the 'classical' $I_{Cl(Ca)}$ recorded in native cells it is interesting to compare the properties of the present Cl^-

channel with these cloned Cl^- channels. Bovine CLCA1 forms Cl^- channels with a conductance of around 30–50 pS when activated by $[Ca^{2+}]_i$ of 5–10 μM and a halide permeability sequence of I^- (2.1) > Cl^- (1.0). (Fuller *et al.* 2001). Although the magnitude of cGMP-activated Ca^{2+}-dependent Cl^- channel conductance in the present study was similar, maximal activation of channels occurred at a much lower $[Ca^{2+}]_i$ of 100 nM and the halide permeability sequence was different (see above). Murine CLCA1 channels expressed in HEK 293 cells had a relative halide permeability of SCN^- (5.3) > Cl^- (1.0) (Britton *et al.* 2002) which is also different from the halide permeability sequence through cGMP-activated Ca^{2+}-dependent Cl^- channels. The sensitivity of cloned CLCA channels to block by niflumic acid appears to depend largely on the expression system. Channels that are expressed in mammalian cell lines are largely blocked by NFA while those expressed in *Xenopus* oocytes are NFA-insensitive (see reviews by Gruber *et al.* 2000; Fuller *et al.* 2001; Jentsch *et al.* 2002; Nilius & Droogmans, 2003). In the present study cGMP-activated Ca^{2+}-dependent Cl^- channels in rat mesenteric artery smooth muscle cells are not blocked by NFA (see above). Therefore, although the electrophysiological data for CLCA channels is rather limited it appears clear that the cGMP-activated Ca^{2+}-dependent Cl^- channels described in the present study are very different to the Cl^- channels encoded by CLCA genes.

The second major class of Ca^{2+}-dependent Cl^- channels to be identified and cloned is the bestrophins. Bestrophin Cl^- channels cloned from *Xenopus laevis* and expressed in HEK 293 cells have a K_d for Ca^{2+} binding of around 200 nM (Qu *et al.* 2003). Increases in $[Ca^{2+}]_i$ produce a graded increase in bestrophin Cl^- current, in contrast to the relationship between $[Ca^{2+}]_i$ and NP_o for cGMP- and Ca^{2+}-dependent channels, which was rather steep. The halide permeability sequence for human bestrophin Cl^- channels was I^- > Cl^- (Sun *et al.* 2002) and for *Xenopus* bestrophin Cl^- channels was also I > Cl^- (Qu *et al.* 2003). The unitary conductance of bestrophin channels has not been determined but nevertheless it appears unlikely that bestrophin Cl^- channels are the molecular correlate of the cGMP- and Ca^{2+}-dependent Cl^- channels described in the present study.

Role of cGMP-dependent protein kinase in Cl^- channel activation

In cell-attached patches from rat mesenteric smooth muscle cells, the addition of the cGMP-dependent kinase (PKG) inhibitor KT5823 reduced the single channel mean open probability, and in inside-out patches inhibition of kinase activity by substitution of ATP by the non-hydrolysable analogue AMP-PNP reduced single channel NP_o. Conversely, activation of PKG by the cGMP analogue 8Br PET cGMP increased the mean single channel open probability and therefore these data indicate that the activation of a PKG may be essential for channel activation. PKG exists in two forms, PKG I which is soluble and is mostly found in the cell cytosol and PKG II which is associated with the plasma membrane (Lohmann *et al.* 1997). In the present study, it is most likely that PKG II is involved in the activation of Cl^- channels, as single channel currents were observed in excised patches, both in the outside-out and inside-out patch configuration. This means that it is likely that the K_d values and n_H for cGMP-dependent activation of Cl^- channels calculated in the present study represent cGMP binding to membrane-bound PKG II, and not to the Cl^- channel itself. PKG II has been shown to be associated with and can phosphorylate and activate the cystic fibrosis transmembrane regulator (CFTR) Cl^- channel (Lohmann *et al.* 1997), therefore it is possible that PKG II forms a similar association with the Cl^- channels described in the present study.

Conclusion

The present study has described the single channel properties of a novel cGMP-activated and Ca^{2+}-dependent Cl^- channel present in rat mesenteric artery smooth muscle cells. Peng *et al.* (2001) have described a cGMP- and Ca^{2+}-dependent inward current in rat mesenteric artery that could be activated by NA and initiated oscillations of vascular tone (vasomotion). A second study from the same group described whole-cell cGMP and Ca^{2+}-dependent Cl^- currents (Matchkov *et al.* 2003), although the reported permeability sequence was I^- > Cl^- > SCN^-. While the properties of the single channels described in this study indicate that they may underlie the cGMP- and Ca^{2+}-dependent inward current in rat mesenteric artery involved in vasomotion (Peng *et al.* 2001), the apparent difference in the halide permeability sequence requires further study.

References

Britton FC, Ohya S, Horowitz B & Greenwood IA (2002). Comparison of the properties of CLCA1 generated currents and $I_{Cl(Ca)}$ in murine portal vein smooth muscle cells. *J Physiol* **539**, 107–117.

Fuller CM, Ji HL, Tousson A, Elble RC, Pauli BU & Benos DJ (2001). Ca^{2+}-activated Cl^- channels: a newly emerging anion transport family. *Pflugers Arch* **443**, S107–S110.

Greenwood IA & Large WA (1999). Modulation of the decay of Ca^{2+}-activated Cl^- currents in rabbit portal vein smooth muscle cells by external anions. *J Physiol* **516**, 365–376.

Gruber AD, Fuller CM, Elble RC, Benos DJ & Pauli BU (2000). The CLCA gene family: a novel family of putative chloride channels. *Curr Genomics* **1**, 201–222.

Hogg RC, Wang Q & Large WA (1994). Action of niflumic acid on evoked and spontaneous calcium-activated chloride and potassium currents in smooth muscle cells from rabbit portal vein. *Br J Pharmacol* **112**, 977–984.

Jentsch TJ, Stein V, Weinreich F & Zdebik AA (2002). Molecular structure and physiological function of chloride channels. *Physiol Rev* **82**, 503–568.

Large WA, Greenwood IA & Piper AS (2002). Recent advances on the properties and role of Ca^{2+}-activated chloride currents in smooth muscle. In *Current Topics in Membranes*, vol. 53, pp. 95–114. Elsevier Science, USA.

Large WA & Wang Q (1996). Characteristics and physiological role of the Ca^{2+}-activated Cl^- conductance in smooth muscle. *Am J Physiol* **268**, C435–C454.

Lohmann SM, Vaandrager AB, Smolenski A, Walter U & De Jong HR (1997). Distinct and specific functions of cGMP-dependent protein kinases. *Trends Biochem Sci* **22**, 307–312.

Matchkov V, Aalkjaer C & Nilsson H (2003). Novel cGMP-dependent calcium-activated chloride current from the mesenteric resistance artery. *J General Physiol* **122**, 93P.

Nilius B & Droogmans G (2003). Amazing chloride channels: an overview. *Acta Physiol Scand* **177**, 119–147.

Peng H, Matchkov V, Ivarsen A, Aalkjaer C & Nilsson H (2001). Hypothesis for the initiation of vasomotion. *Circ Res* **88**, 810–815.

Piper AS, Greenwood IA & Large WA (2002). Dual effect of blocking agents on Ca^{2+}-activated Cl^- currents in rabbit pulmonary artery smooth muscle cells. *J Physiol* **539**, 119–131.

Piper AS & Large WA (2003). Single Ca^{2+}-activated Cl^- channels in rabbit isolated pulmonary artery smooth muscle cells. *J Physiol* **547**, 181–196.

Qu Z, Wei RW, Mann W & Hartzell HC (2003). Two bestrophins cloned from *Xenopus laevis* oocytes express Ca-activated Cl currents. *J Biol Chem* **278**, 49563–49572.

Sun H, Tsunenari T, Yau K-W & Nathans J (2002). The vitelliform macular dystrophy protein defines a new family of chloride channels. *Proc Natl Acad Sci U S A* **99**, 4008–4013.

Acknowledgement

This work was supported by The Wellcome Trust.